

# INFRARED OBSERVATIONS OF ASTEROIDS\*

DENNIS L. MATSON  
*California Institute of Technology*

*This paper is a brief preliminary report about a program of reconnaissance photometry designed to study the thermal radiation emitted from asteroids. Observations of thermal radiation, and their subsequent interpretation, can provide new knowledge that presently cannot be gained by any other method. The emitted thermal power is by and large that portion of the insolation which is absorbed. Part of the asteroid's emission spectrum can be observed through windows in Earth's atmosphere. With the aid of models for the details of energy transfer at the asteroid's surface, and accurate visual photometry, reliable estimates can be made for some of the important parameters in the models. Of particular interest are Bond albedo, size, emissivity, and thermal inertia.*

Infrared observations were made through bandpasses centered at 8.5, 10.5, and 11.6  $\mu\text{m}$  ( $\Delta\lambda = 0.5, 0.5, \text{ and } 1.0 \mu\text{m}$ , respectively). The observations were made from July 21, 1969, to July 27, 1970, using the Hale Observatories' 1.52 m telescope at Mt. Wilson. A total of 26 objects was observed: 1 Ceres, 2 Pallas, 3 Juno, 4 Vesta, 5 Astraea, 6 Hebe, 7 Iris, 8 Flora, 9 Metis, 15 Eunomia, 16 Psyche, 18 Melpomene, 19 Fortuna, 20 Massalia, 25 Phocaea, 27 Euterpe, 39 Laetitia, 44 Nysa, 68 Leto, 80 Sappho, 145 Adeona, 163 Erigone, 192 Nausikaa, 313 Chaldaea, 324 Bamberga, and 674 Rachele. Most of the program asteroids were observed through the 11.6  $\mu\text{m}$  bandpass, and bright objects were measured at all three wavelengths. The observational coverage varies from good for the bright objects, which were observed at a number of phase angles, to poor for those asteroids observed only once.

Phase data for 4 Vesta and 7 Iris are shown in figures 1 and 2. Each point represents the weighted nightly mean. The curve in each of these figures is the average using both the 4 Vesta and 7 Iris data. This curve is used to correct all the 11.6  $\mu\text{m}$  thermal emission observations to zero phase angle. For any given angle, the phase variation is a function of the temperature distribution, which in turn is a function of the thermal properties of the asteroidal surface, the orbit, the rotational period, and the aspect geometry. The regions on each side of opposition where the phase angle is large are the two most important critical regions for testing thermal models. Under the proper circumstances, additional

---

\*This paper is contribution no. 2039 of the Division of Geological and Planetary Sciences.

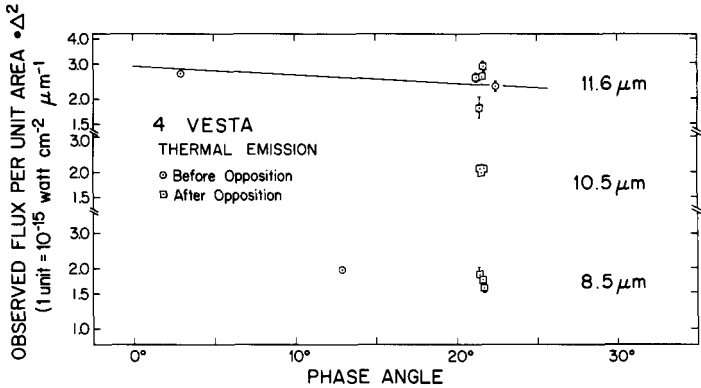


Figure 1.—Phase data for 4 Vesta. The curve through the 11.6  $\mu\text{m}$  data is the phase function used for the reduction of the data presented in figure 3. Errors for some of the data are less than the size of the plotted symbol. Allen's (1970) data for the same opposition have not yet been reduced to the present photometry systems.

critical regions can be provided by aspect differences from one opposition to another.

The ordinate on the phase plots is calibrated by the assumption that  $\alpha$ -Bootis has a flux per unit area at Earth of 4.1, 1.8, and  $1.2 \times 10^{-15}$   $\text{W}\cdot\text{cm}^{-2}$  per micrometer for 8.5, 10.5, and 11.6  $\mu\text{m}$ , respectively. The accuracy of this calibration is not known. The calibrations currently for use in the 8 to 14  $\mu\text{m}$  region have a range of about 20 percent.

All measurements reported here were made with respect to three new stellar photometry systems that were established from observations obtained concurrently with the asteroid program and using the same equipment (Matson, 1971).

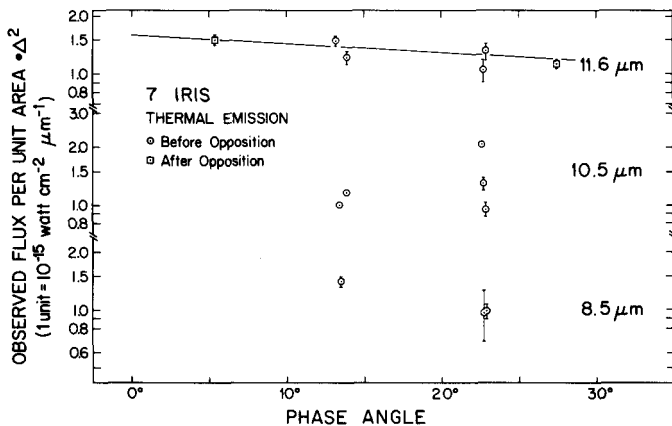


Figure 2.—Phase data for 7 Iris. Some of the scatter is due to the lightcurve.

The scatter shown by the 7 Iris data is due to the lightcurve variation of that asteroid. In fact, enough data are available to construct a composite lightcurve of the thermal emission at 10.5  $\mu\text{m}$ . Correlation of these data with the phase of the visible lightcurve will enable one to differentiate between a spotted asteroid and an irregularly shaped object. This can also be accomplished with the infrared data alone by using observations from two bandpasses to obtain the color temperature as a function of the rotational phase angle. For this method the propagation of observational errors is not as favorable as when using the visible and infrared data.

The error bars on the two phase variation plots represent the propagation of all random and nominal errors incurred in transferring the asteroid observation to  $\alpha$ -Bootis. The bounds are intended to delimit the region where the probability of the "true value" is two-thirds or greater.

Table I tabulates some simple models that have been used to analyze the same 4 Vesta data. The parameters, as it can be seen, vary as the model is changed. The common assumption of the three models in table I is that each elemental area on the surface radiates like a blackbody. Phase effects, other than for the corrections applied to the observational data, have been ignored. The albedo parameter has been assumed to be independent of wavelength. This parameter is a weighted average over the solar spectrum. The weight is the amount of energy absorbed at each wavelength.

TABLE I.—*Simple Models for 4 Vesta*

Description	Method of handling temperature $T$ distribution	Model albedo	Model radius, km
Flat disk	$T = \text{constant}$	0.13	264
Smooth, nonrotating sphere	$T = \left[ \frac{(1 - a)S \cos \phi}{\sigma} \right]^{1/4}$	.085	328
"Rough," nonrotating sphere	$T = \left[ \frac{(1 - a)S}{\sigma} \right]^{1/4} (\cos \phi)^{1/6}$	.098	306

$\sigma$  = Stefan-Boltzmann constant;  $\phi$  = angle between heliocentric radius vector and local surface normal; and  $S$  = solar constant at the asteroid.

The albedos provided by the models are surprisingly low and the corresponding sizes are large compared to disk measurements. The models and the absolute calibration of the photometry have a systematic error of unknown size and it is premature to assume that the albedo anomaly is due to some unexpected property of asteroidal surfaces. Currently, detailed thermal models that take rotation and the direction of the pole into account are being examined. The simple models (table I) err chiefly in their treatment of the

infrared phase integral and are used only for a differential comparison of the data.

Table I shows that the changes in parameters from model to model are small enough that it is safe to draw some conclusions at this time. For this purpose, the "rough," nonrotating sphere model is employed because it represents the Moon better than the other two. Normalization to 4 Vesta enables a differential comparison to be made between asteroids. The arbitrary normalization is set at 210 km radius and 0.3 albedo. In this way systematic errors from many diverse sources are mitigated, but other errors are introduced. For example, error from the visible phase integral  $q$  for 4 Vesta is introduced if the result is interpreted as the Bond albedo. The  $11.6 \mu\text{m}$  infrared data are corrected to zero phase angle, and the visible data,  $B(1, 0)$ , are taken from Gehrels (1970). The resulting model radius and model albedo are plotted in figure 3.

The first things to note are the infrared points for 1 Ceres and 2 Pallas. Already they are in reasonable agreement with published data. Part of the difference is the result of the adopted normalization and the model.

The asteroids vary in the albedo parameter from about 0.03 for 324 Bamberga to about 0.3 for several objects. 324 Bamberga is extremely dark. Presently it is the darkest member of a group of large, dark asteroids. By contrast, 4 Vesta appears to be unique—the only known large, light-colored asteroid. Objects of comparable albedo are not encountered until the 50 to 90 km radius interval is reached. Type I bias is the discrimination against small,

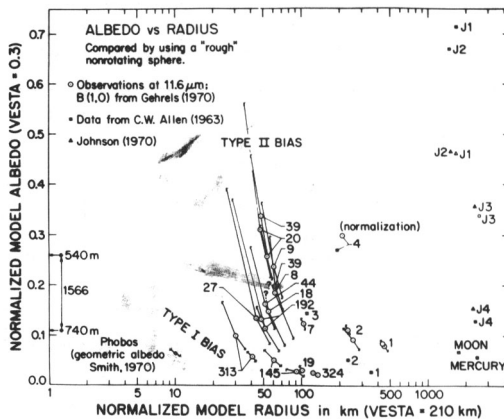


Figure 3.—Differential comparison of the model parameters for selected asteroids. The error bars are for the infrared photometry only. The errors in albedo and radius are correlated and lie along trajectories defined by  $B(1, 0) = \text{constant}$ . Errors in  $B(1, 0)$  and the phase correction are not plotted. The lightcurves appear to be responsible for much of the scatter of values for the smaller asteroids. The ordinate for the data from the literature is the Bond albedo, which is approximately equivalent to the normalized model albedo. Data for Icarus is from Gehrels et al. (1970) and Veverka and Liller (1969).

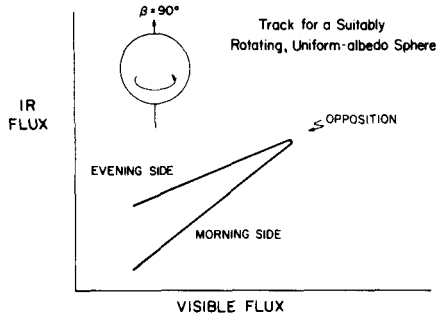


Figure 4.—Infrared flux as a qualitative function of visible flux for a rotating, spherical minor planet with uniform albedo and zero obliquity.

dark asteroids. 313 Chaldaea was obtained near the end of the program when a small number of objects that were thought to be too faint for detection were observed. Considering this bias, it seems likely that there exist small, dark asteroids comparable in size and albedo to Phobos. Infrared observations of Phobos are extremely important. This control point will help to remove distortion in the radius and albedo scales due to differences in surface morphology between large and small asteroids.

At the other extreme of the albedo range is type II bias. Here objects are unduly favored by observational selection. It is surprising that more of them were not discovered. This implies that they are not particularly abundant in the time and space regions sampled.

At this time 20 Massalia and 39 Laetitia are the asteroids with the highest albedo. Their data are dispersed because of their lightcurves. In this reduction, their albedo is in the same class as 4 Vesta and perhaps J3, using Johnson's (1970) lunar-model values for the Bond albedo.

For the large bodies without atmospheres, the trend in the inner part of the solar system is one of low albedo. The Moon, Mercury, and perhaps J4 can be thought of as part of a branch of large, dark objects. The light objects appear to be singular with no trend except for the sheer size of the Galilean satellites of Jupiter. At a radius of about 100 km the dark asteroids continue but they are now joined by objects with higher albedos.

Considering the errors in the model and in the data, it would be risky to draw conclusions about any of the smaller features of figure 3.

Infrared observations also have other applications that are not related to the main thrust of this project. For example, they can aid in the study of rotating asteroids. Consider a rotating, spherical asteroid with an absolutely uniform albedo. Figure 4 shows how the visible and infrared fluxes will be related. Before opposition, warm material is still seen after it crosses the evening terminator. After opposition, the morning terminator of the asteroid is viewed and cool material on the night side contributes only a small amount to the infrared radiation.

### ACKNOWLEDGMENTS

The author thanks Bruce C. Murray for suggestions, encouragement, and discussions throughout the course of this project. Gordon Hoover assisted with all of the observations and was indispensable to the program. A special thanks goes to the staff of the Hale Observatories for the many courtesies that they rendered. This work was supported by the National Aeronautics and Space Administration Grant NGL 05-002-003.

### REFERENCES

- Allen, C. W. 1963, *Astrophysical Quantities*. Athlone Press. London.
- Allen, David A. 1970, Infrared Diameter of Vesta. *Nature* **227**, 158-159.
- Gehrels, T. 1970, Photometry of Asteroids. Surfaces and Interiors of Planets and Satellites (ed., Dollfus), ch. 6, pp. 317-375. Academic Press, Inc. New York.
- Gehrels, T., Roemer, E., Taylor, R. C., and Zellner, B. H. 1970, Minor Planets and Related Objects. IV. Asteroid (1566) Icarus. *Astron. J.* **75**, 186-195.
- Johnson, Torrence Vano. 1970, Albedo and Spectral Reflectivity of the Galilean Satellites of Jupiter, p. 58. Ph. D. Thesis, Calif. Inst. of Tech.
- Matson, D. L. 1971, Ph. D. Thesis, in preparation.
- Smith, Bradford A. 1970, Phobos: Preliminary Results From Mariner 7. *Science* **168**, 828-830.
- Veverka, J., and Liller, W. 1969, Observations of Icarus: 1968. *Icarus* **10**, 441-444.

### DISCUSSION

**ANONYMOUS:** What happens to the albedo as the size decreases?

**MATSON:** As the slide showed, we continue to get dark objects but we also seem to be seeing lighter objects at a model radius of about 60 km. Although we say there are some lighter objects, I could not really say which ones because I am worried about the extent of the lightcurve variation of these small objects.

**ANONYMOUS:** It would seem to me that the type of model that you consider should take into account the scattering properties of the surface material. Is this being done?

**ALLEN:** This is fairly ineffective. I think one cannot as yet try to arrive at any conclusions. Roughness and shape are the most important things and if we ultimately get accurate diameters, from some other method, and we only have two unknowns left, then eventually it can be solved—but not yet.

**ANONYMOUS:** What if the emissivities are not unity?

**MATSON:** For the brighter objects there are things that can be done (using observations at three wavelengths), and I am running models for Vesta that are fairly sophisticated in order to check. But for those asteroids with radii of less than 100 km I do not have much hope for improving the situation with the present data. For the smaller objects there is currently data at only 11.6  $\mu\text{m}$ . With future observations we may be able to work out some of the difficulties.